Mon. Not. R. Astron. Soc. **285,** 811–819 (1997)

Growth of density perturbations with a cosmological constant

Reuven Opher, Nilza Pires★ and José Carlos N. de Araujo

Instituto Astronômico e Geofísico, Universidade de São Paulo, Av. Miguel Stefano, 4200, 04301-904, São Paulo, SP, Brazil

Accepted 1996 October 20. Received 1996 August 28; in original form 1996 March 1

ABSTRACT

We investigate the influence both of the cosmological constant and of the physical processes that take place during the evolution of the Universe on the primordial cloud collapse. We study the evolution of a cloud with a density perturbation, δ, from the recombination era to the present. As an example, we study an initial perturbation $\delta_i = 10^{-6}$ for a cloud of mass 10^4, 10^5 and 10^6 $M_\odot$. In particular, we study the influence of the physical processes on the evolution of the peculiar velocity factor, $f = d \ln \delta / d \ln a$, where '$a$' is the scalefactor of the Universe. We compare our results with the analytic expression for f obtained by Lahav et al. Our results show that the physical mechanisms (photon drag, photon cooling, recombination, etc.) amplify perturbations, and the cosmological constant is particularly important in a Universe dominated by it with a small matter density.

Key words: cosmology: theory – early Universe – large-scale structure of Universe.

1 INTRODUCTION

In a Friedmann–Robertson–Walker Universe, we can write

$$\Omega_T = \Omega + \lambda = 1 - \Omega_k. \quad (1)$$

where

$$\Omega = \frac{8\pi G}{3H^2}\rho, \qquad \lambda = \frac{\Lambda}{3H_0^2}$$

and

$$\Omega_k = -\frac{k}{a^2 H^2},$$

$H = \dot{a}/a$, a and $\dot{a}$ being the scalefactor and the time derivative of the scalefactor, respectively, with $a/a_0 = (1+z)^{-1}$. z is the redshift, $\rho = \rho_0 (a_0/a)^3$ is the ambient matter density, and Λ (or λ) is called the cosmological constant. We have $k = -1$ for an open universe, $k = 0$ for a flat universe and $k = +1$ for a closed universe. The zero subscript designates the present-day value.

The infall velocity of a supercluster has been used to compute the density parameter Ω_0 and the cosmological constant λ (Davis et al. 1980). It is related to the peculiar velocity factor, f, that gives the relation between the peculiar velocity and the peculiar acceleration of the density perturbation in linear theory (Peebles 1980, section 14).

Likewise, it has been shown (e.g. Peebles 1984; Lightman & Schechter 1990; Martel 1991) that the present infall velocity is almost entirely determined by Ω_0, with a very weak dependence on λ. However, Lahav et al. (1991, hereafter LLPR), as well as Barrow & Saich (1993), showed that this is true at the present epoch, but for redshifts in the range 0.5–2.0, the peculiar velocity is much more sensitive to λ than to Ω_0.

It is important to note that all studies (spherical infall: Peebles 1984, Martel 1991 and LLPR; non-spherical infall: Barrow & Saich 1993) without taking into account dark matter, were made considering only the linear theory of the perturbations and did not take into account the various physical processes (except gravitation) that were significant in the evolution of the perturbation.

The main motivation for this paper is to compare the peculiar velocity factor, f, deduced by the linear theory, first by Peebles (1980) for $z = 0$ and then by LLPR for any z, λ, and Ω_0, with the exact calculations of the hydrodynamical equations, taking into account the effects of a non-zero cosmological constant and the physical mechanisms that were present during and after the recombination era upon the peculiar velocity field evolution, as well as the amplification of the density perturbations since the recombination era. The physical processes that we take into account are

★On leave from the Departamento de Física Teórica e Experimental, UFRN, Campus Universitário, 59072-970, Natal, RN, Brazil

photon drag, photon cooling, recombination, photoionization, collisional ionization, and hydrogen molecule production, destruction and cooling – hereafter called simply 'physical mechanisms'. The basic equations and calculations were presented in various papers of de Araujo & Opher (1988, 1989, 1990, 1994). We modified the code developed by de Araujo (1990) to perform the calculations in this paper. The present paper differs from the LLPR paper by the inclusion of the 'physical mechanisms' and also differs from the LLPR paper in the initial conditions. In the LLPR paper, only the growing solution was used. In the present paper we use the general solution (the sum of the growing and decaying solutions). The general solution is normalized with the condition that the time derivative of the perturbation is zero at the beginning of the recombination era.

We give the basic hydrodynamical equations and the physical processes used in Section 2. In Section 3 we give a brief review of the peculiar velocity field and the results that we obtained regarding the peculiar velocity factor. Section 4 gives the amplification of the density perturbation that we discovered. The results and discussions are given in Section 5, and in the last section we give the main conclusions that we obtained.

2 THE BASIC EQUATIONS AND THE MODEL

The basic equations used (cf. de Araujo & Opher 1988, 1989, 1990, 1994) are

$$\frac{\partial\rho}{\partial t}+\nabla\cdot(\rho\boldsymbol{v})=0, \tag{2}$$

the continuity equation, and

$$\frac{\mathrm{d}\boldsymbol{v}}{\mathrm{d}t}=-\nabla\phi-\frac{1}{\rho}\nabla P-\frac{\sigma bT_{\mathrm{r}}^{4}\chi_{e}}{m_{p}c}(\boldsymbol{V}-H\boldsymbol{r}), \tag{3}$$

the equation of motion, where σ is the Thomson cross-section, $b=4/c$ the Stefan–Boltzmann constant, and T_{r} the radiation temperature. The last term in equation (2) is the term of photon drag arising from the background cosmic radiation. The degree of ionization χ_e is given by Peebles (1968), modified to include collisional ionization. The field equation (Poisson's equation) is

$$\nabla^{2}\phi=4\pi G\rho-\Lambda. \tag{4}$$

The equation of state is given by

$$P=Nk_{\mathrm{B}}\rho(1+\chi_{e})\,T_{\mathrm{m}}, \tag{5}$$

where T_{m} is the matter temperature, k_{B} the Boltzmann constant, and N the Avogadro number. For the energy equation, we have

$$\frac{\mathrm{d}U}{\mathrm{d}t}=-L+\frac{P}{\rho^{2}}\frac{\mathrm{d}\rho}{\mathrm{d}t}, \tag{6}$$

where L is the cooling function and U is the energy density per unit mass of baryonic matter, given by

$$U=\frac{3}{2}Nk_{\mathrm{B}}T_{\mathrm{m}}(1+\chi_{e}), \tag{7}$$

neglecting the contribution of hydrogen molecules.

For the cooling function of the baryonic matter we have:

$$L=-Nk_{\mathrm{B}}T_{\mathrm{m}}\dot{\chi}_{e}+\frac{4\sigma bT_{\mathrm{r}}^{4}Nk_{\mathrm{b}}}{m_{e}c}\chi_{e}(T_{\mathrm{m}}-T_{\mathrm{r}})+L_{\mathrm{H_2}}+L_{\mathrm{L_\alpha}}, \tag{8}$$

which includes recombination, photoionization and collisional ionization (first term), photon cooling (heating, second term), molecular hydrogen cooling and Lyman-α cooling (third and fourth terms, respectively). $\dot{\chi}_e$ is the time derivative of χ_e.

The hydrogen molecular cooling function ($L_{\mathrm{H_2}}$), taken from Lepp & Shull (1983), is good for densities $n>0.1\ \mathrm{cm}^{-3}$ and temperatures $100\ \mathrm{K}<T_{\mathrm{m}}<10^{6}\ \mathrm{K}$. For Lyman-$\alpha$ cooling, $L_{\mathrm{L_\alpha}}$, we use the expression of Carlberg (1981). With the dimensions, densities, and temperatures in the calculations made in this paper, radiative transfer is not important. All the calculations herein have small optical depth.

In order to solve the above equations, we use a top-hat perturbation of mass M_c, with a density ρ_c,

$$\rho_{c}=\rho+\rho_{1}(t)=\rho[1+\delta(t)], \tag{9}$$

where δ is the contrast density, and a linear dependence for the velocity (which is consistent with the density profile)

$$\boldsymbol{v}_{\mathrm{c}}=H\boldsymbol{r}+v_{1}(t)\frac{\boldsymbol{r}}{r_{\mathrm{c}}}, \tag{10}$$

with r_{c} being the radius of the cloud (or perturbation).

The system of equations (equations 2–9) was numerically integrated using the sub-routine IMSL-DVERK (this uses the Runge–Kutta method – see e.g. Press et al. 1992), using HP-Apollo 900 and SUN SPARC2 workstations.

We started the calculations at the beginning of the recombination era $T_{\mathrm{R}}=4000\ \mathrm{K}$ ($z_{\mathrm{R}}\simeq 1482$).

We studied five models, parametrized by Ω_0 and λ, which we refer to as models A–E. They are listed in Table 1. These models were suggested by Carroll, Press & Turner (1992). For each model we analyse clouds of masses 10^4, 10^5 and $10^6\ \mathrm{M}_{\odot}$. As an example, we study an initial perturbation $\delta_{\mathrm{i}}=10^{-6}$, small enough in order to compare with the linear approach.

3 THE PECULIAR VELOCITY FIELD AND THE PECULIAR VELOCITY FACTOR

The peculiar velocity, $\boldsymbol{v}_1$, is related to the peculiar acceleration, $\boldsymbol{g}$, by the peculiar velocity factor f (Peebles 1980, section 14):

$$\boldsymbol{v}_{1}=\frac{Hf\boldsymbol{g}}{4\pi G\rho_{b}}=\frac{2f\boldsymbol{g}}{3H\Omega}, \tag{11}$$

Table 1. The models for Ω_T, Ω_0 and λ, utilized in the calculations ($\Omega_T=\Omega_0+\lambda$).

Model	Ω_T	Ω_0	λ
A	1	1	0
B	0.1	0.1	0
C	1	0.1	0.9
D	0.01	0.01	0
E	1	0.01	0.99

with

$$f=\frac{a}{\delta}\frac{\mathrm{d}\delta}{\mathrm{d}a}=\frac{\mathrm{d}\ln\delta}{\mathrm{d}\ln a}. \tag{12}$$

Starting from the solution of the linearized equation for δ found by Heath (1977), LLPR generalized the calculation of f for any value of Ω_0, λ and redshift z (taking $a_0=1$):

$$f(\Omega_0,\lambda,z)=X^{-1}\left[\lambda(1+z)^{-2}-\frac{\Omega_0}{2}(1+z)\right]$$
$$-1+\frac{(1+z)^{-1}X^{-3/2}}{\int_0^{(1+z)^{-1}}X^{-3/2}\,\mathrm{d}a}, \tag{13}$$

where $(1+z)^{-1}=a$ and $X=1+\Omega_0 z+\lambda[(1+z)^{-2}-1]$. There are two cases for which the solution of equation (13) is analytical: first, when $\Omega_0=1$ and $\lambda=0$, we have $f=1$ for

Table 2. Amplification of an initial perturbation $\delta_i=10^{-6}$ for all the models.

Model	M_n	A_{LLPR}	A_{SF}	A_F
A	10^4	1481	889	4402
A	10^5	1481	889	1993
A	10^6	1481	889	1170
B	10^4	281	172	567
B	10^5	281	172	306
B	10^6	281	172	182
C	10^4	885	525	1566
C	10^5	885	525	923
C	10^6	885	525	574
D	10^4	35	22	79
D	10^5	35	22	41
D	10^6	35	22	21
E	10^4	425	266	136
E	10^5	425	266	591
E	10^6	425	266	335

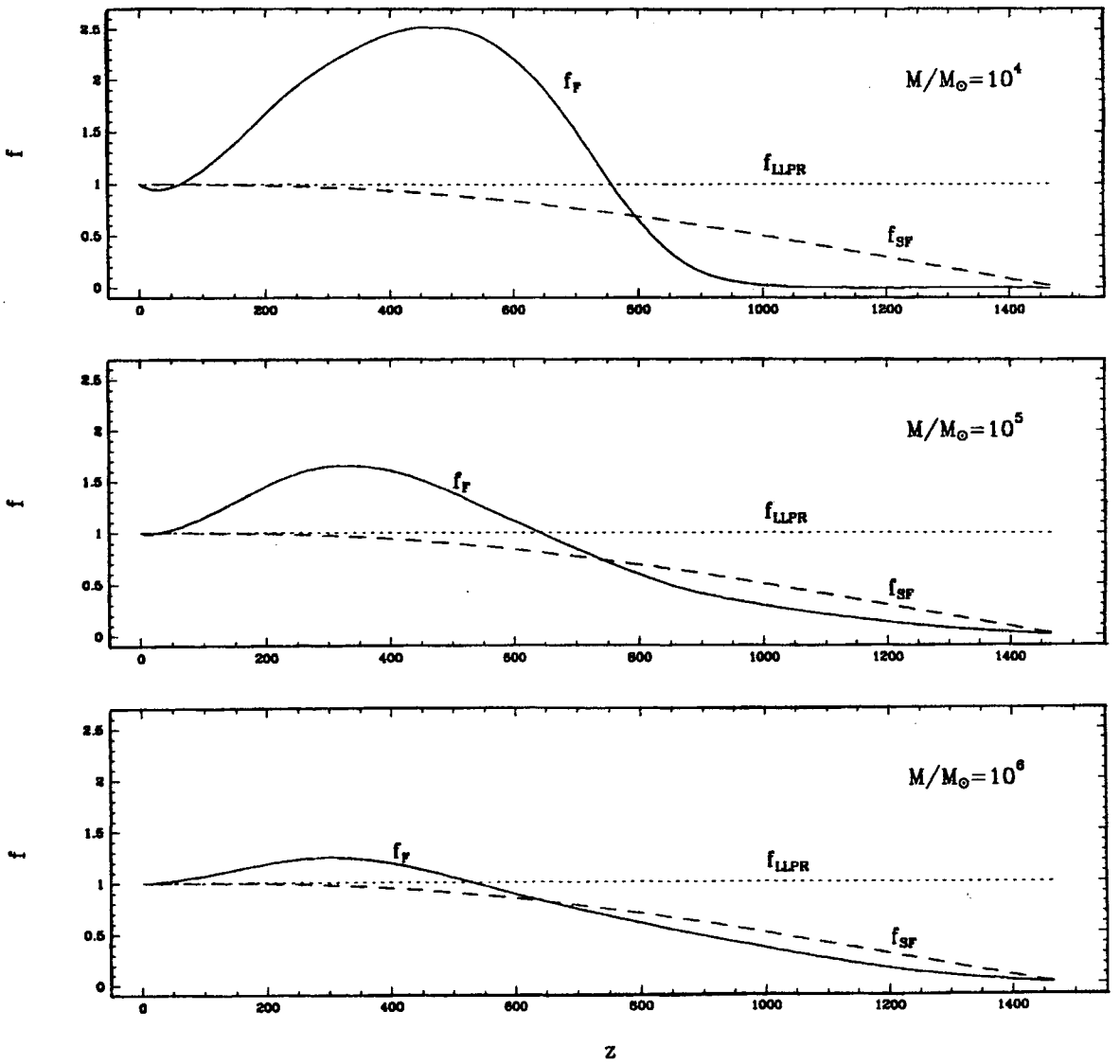

Figure 1. The peculiar velocity factor f versus redshift from the recombination era until the present. The dotted curve is f_{LLPR}, the dashed curve is f_{SF} calculated without physical mechanisms and pressure, and the solid curve is f_F calculated with physical mechanisms. For model A, $\Omega_0=1.0$, $\lambda=0.0$ and $h_0=1.0$.

all z's; secondly, when $\lambda=0$ and $z=0$, the solution can be written in terms of a hypergeometric function,

$$f_0=-\frac{\Omega_0}{2}-1+\frac{5}{2}\frac{\Omega_0^{3/2}}{F(\frac{3}{2},\frac{5}{2},\frac{7}{2},1-\Omega_0^{-1})}. \tag{14}$$

Approximations for equation (14) have appeared in the literature, e.g.

Peebles 1980: $f_0\approx\Omega_0^{0.6}$,

Lightman & Schechter 1990: $f_0\approx\Omega_0^{4/7}$.

Approximations for equation (13) have been made with $\Lambda\neq0$ and $z=0$ for the range $-5\leq\lambda\leq5$ and $0.03\leq\Omega_0\leq2$,

LLPR: $f_0\approx\Omega_0^{0.6}+\frac{\lambda}{70}\left(1+\frac{\Omega_0}{2}\right)$,

Martel 1991: $f_0\approx\Omega_0^{0.6}+\frac{\lambda}{30}$.

These approximations show that for $z=0$, f is almost entirely determined by Ω_0, with a very small dependence on λ.

LLPR found an approximate formula valid for all z, λ and Ω_0:

$$f_{\rm LLPR}=\left[\frac{\Omega_0(1+z)^3}{\Omega_0(1+z)^3-(\Omega_0+\lambda-1)(1+z)^2+\lambda}\right]^{4/7}. \tag{15}$$

They found that for $z>0$, f is more sensitive to λ than to Ω_0; in particular, in the interval $z\approx0.5$–2.0 it is possible to discriminate between universes with different cosmological parameters.

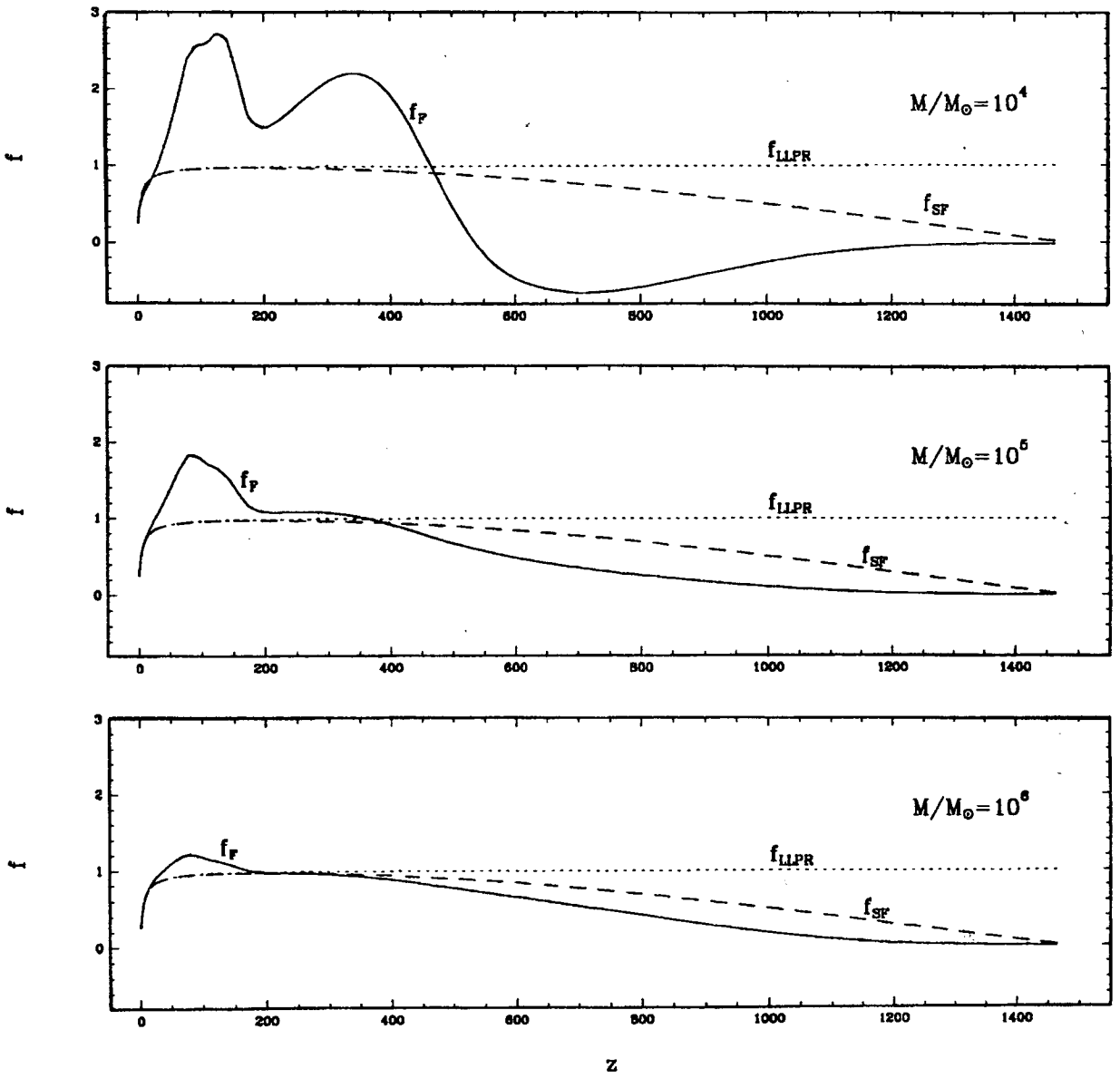

Figure 2. Same as Fig. 1 but for model B, where $\Omega_0=0.1$, $\lambda=0.0$ and $h_0=1.0$.

4 AMPLIFICATION OF THE DENSITY PERTURBATIONS

The amplification of the density perturbation, δ, from the beginning of the recombination era [$\delta(t_R)$] to the present [$\delta(t_0)$] for growing modes (designated by a '+' subscript) is

$$A \equiv \frac{\delta_+(t_0)}{\delta_+(t_R)} = \frac{\delta_0}{\delta_R}. \tag{16}$$

We made the calculation with and wtihout the physical mechanisms.

In order to calculate the amplification by LLPR, we take the equations given by LLPR and, after some manipulation, find

$$A_{\rm LLPR}\left(=\frac{\delta_0}{\delta_R}\right) = \frac{X_R(1+f_R) - \lambda a_R^2 + \Omega_0/2a_R}{X_0(1+f_0) - \lambda a_0^2 + \Omega_0/2a_0}, \tag{17}$$

where $X_j = 1 + \Omega_0(a_j^{-1} - 1) + \lambda(a_j^2 - 1)$ and $f_j = \{\Omega_0(1+z_j)^3/[\Omega_0(1+z_j)^3 - (\Omega_0 + \lambda - 1)(1+z_j)^2 + \lambda]\}^{4/7}$, $j = 0$ means the present and $j = R$ the recombination era.

Our amplification, when physical mechanisms are taken into account, is evaluated directly from equation (16).

In linear theory there are two solutions of the perturbation equation: a growing solution, δ_+, and a damped solution, δ_-. It is usual to use only the solution δ_+ to calculate the amplification. Our numerical solution calculated with our code is for the general solution $\delta = C_1\delta_+ + C_2\delta_-$, indicating the need to find the values of the proportionality constants. We do this by making the reasonable assumption that at the recombination era, the temporal derivative of δ is zero.

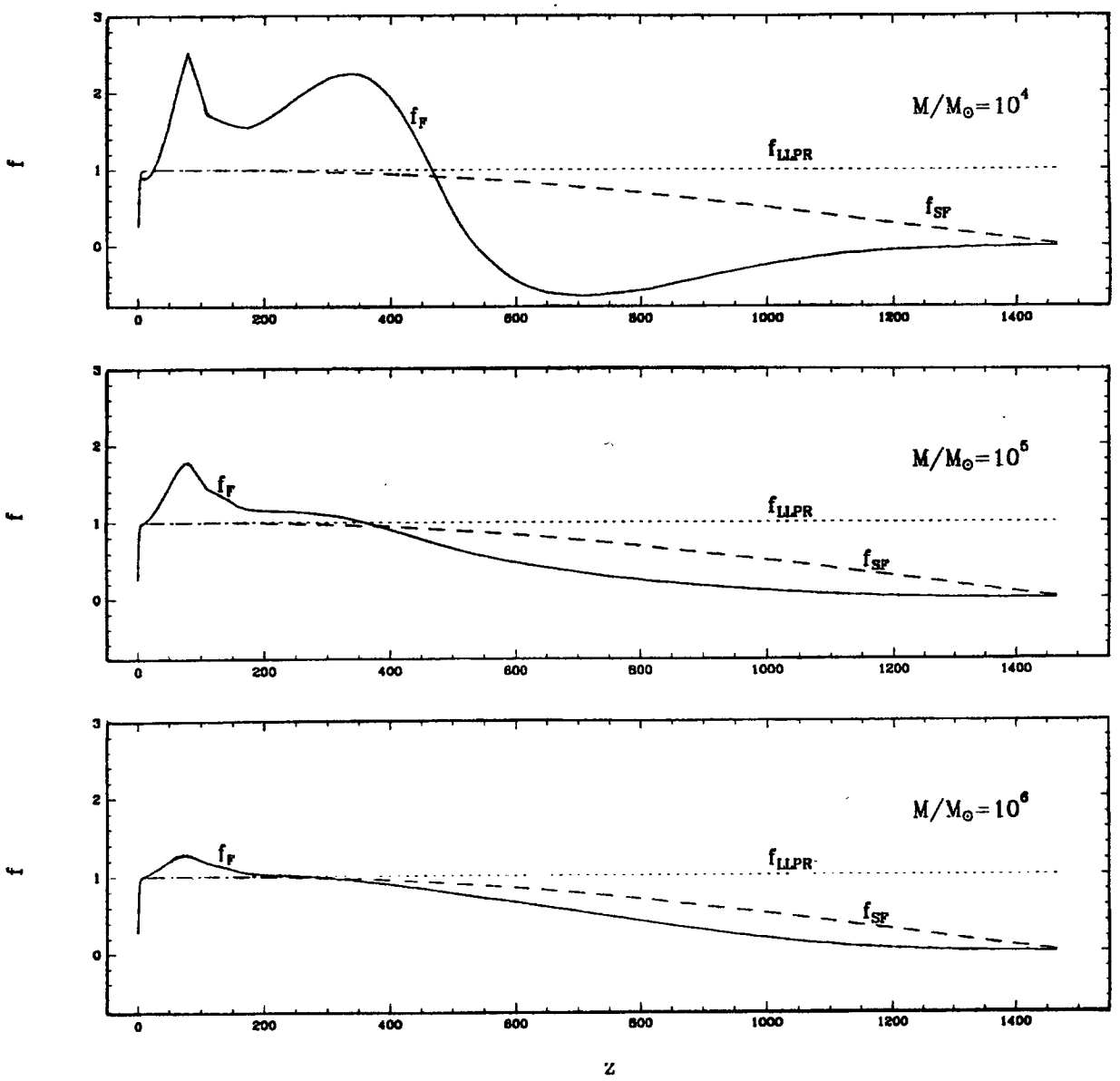

Figure 3. Same as Fig. 1 but for model C, where $\Omega_0 = 0.1$, $\lambda = 0.9$ and $h_0 = 1.0$.

For example, in the case where $k=0$ (flat), $\lambda=0$, and without physical mechanisms, it is easy to show that in this case the general solution is

$$\delta(z)=C_1(1+z)^{2/3}+C_2(1+z)^{-1}, \tag{18}$$

with

$$C_1=\frac{3(1+z_r)}{5}\delta_R=889\delta_R, \tag{19}$$

and

$$C_2=\frac{2(1+z_R)^{-3/2}}{5}\delta_R=7.0\times10^{-6}\delta_R, \tag{20}$$

where we assume $z_R\approx1482$.

In Table 2 we have: (1) A_{LLPR} (from equation 17); (2) A_{SF} (numerical calculation without physical mechanisms); and (3) A_F (our numerical calculation of the amplification, taking into account the physical mechanisms).

The comparison between A_{LLPR} with A_{SF} shows that A_{LLPR} is bigger than A_{SF}. This is because LLPR evaluated the amplification using only the growing numerical solution, i.e. $C_1\delta_+$. We note that the value for the amplification used for the simple case of just the growing solution where $k=0$ and $\lambda=0$ is $1+z_R$ (see Weinberg 1972).

Table 2 shows clearly, from A_F, that the amplification of the perturbation δ_i has a strong dependence on the physical mechanisms.

For the model that is matter dominated (i.e. model A), the amplification A_F is bigger than A_{SF} or A_{LLPR}. Comparing model B ($\Omega_0=0.1$, $\lambda=0$) with model C ($\Omega_0=0.1$, $\lambda=0.9$),

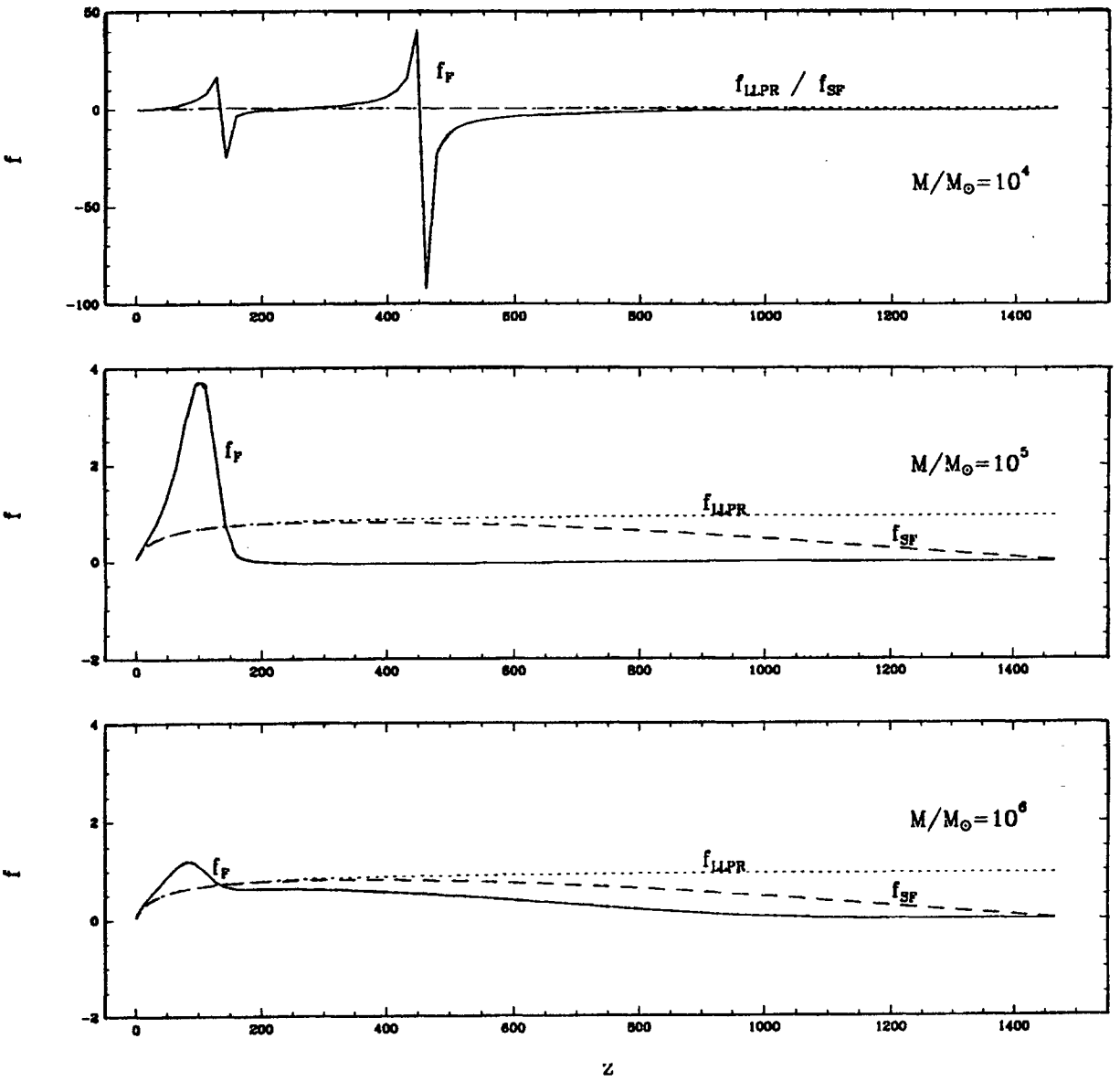

Figure 4. Same as Fig. 1 but for model D, where $\Omega_0=0.01$, $\lambda=0.0$ and $h_0=1.0$.

model D ($\Omega_0=0.01$, $\lambda=0$) and model E ($\Omega_0=0.01$, $\lambda=0.99$), we find that the presence of a cosmological constant increases the amplification.

Comparing A_F with A_{SF} there is seen to be a coupling between the cosmological constant and the physical mechanisms.

5 RESULTS AND DISCUSSION OF THE PECULIAR VELOCITY FACTOR

Figs 1–5 show the peculiar velocity factor, f, versus redshift z from the beginning of the recombination era until the present. The dotted curve is equation (15), f_{LLPR}; the dashed curve is f_{SF}, calculated numerically without physical mechanisms and pressure; and the solid curve is f_F, calculated taking into account the physical mechanisms.

At a first glance we can see that the three curves differ significantly. Again, as discussed in the last section, the difference between f_{LLPR} and f_{SF} is a result of the use of the general numerical solution (i.e. $C_1\delta_+ + C_2\delta_-$) in the calculation of f_{SF} (besides the inclusion of the physical mechanisms). Of course, we use the general solution for the evaluation of f_F as well. We note that we obtain the same results (f_{LLPR} versus f_{SF}) as LLPR if the physical processes are turned off and the initial conditions are the same.

As we discussed in the last section, in order to analyse the importance of the physical mechanisms, we need to compare f_{SF} (dashed curve) with f_F (solid curve). In particular, the physical mechanisms are important for $z \gtrsim 10$.

Figs 1–5 show that there exists a general trend in the behaviour of the curve f_F. We observe, starting from the recombination era until the present, that the physical mechanisms first push f_F below f_{SF} until a minimum, after the minimum it increases up to f_{SF}, surpasses f_{SF} and reaches a

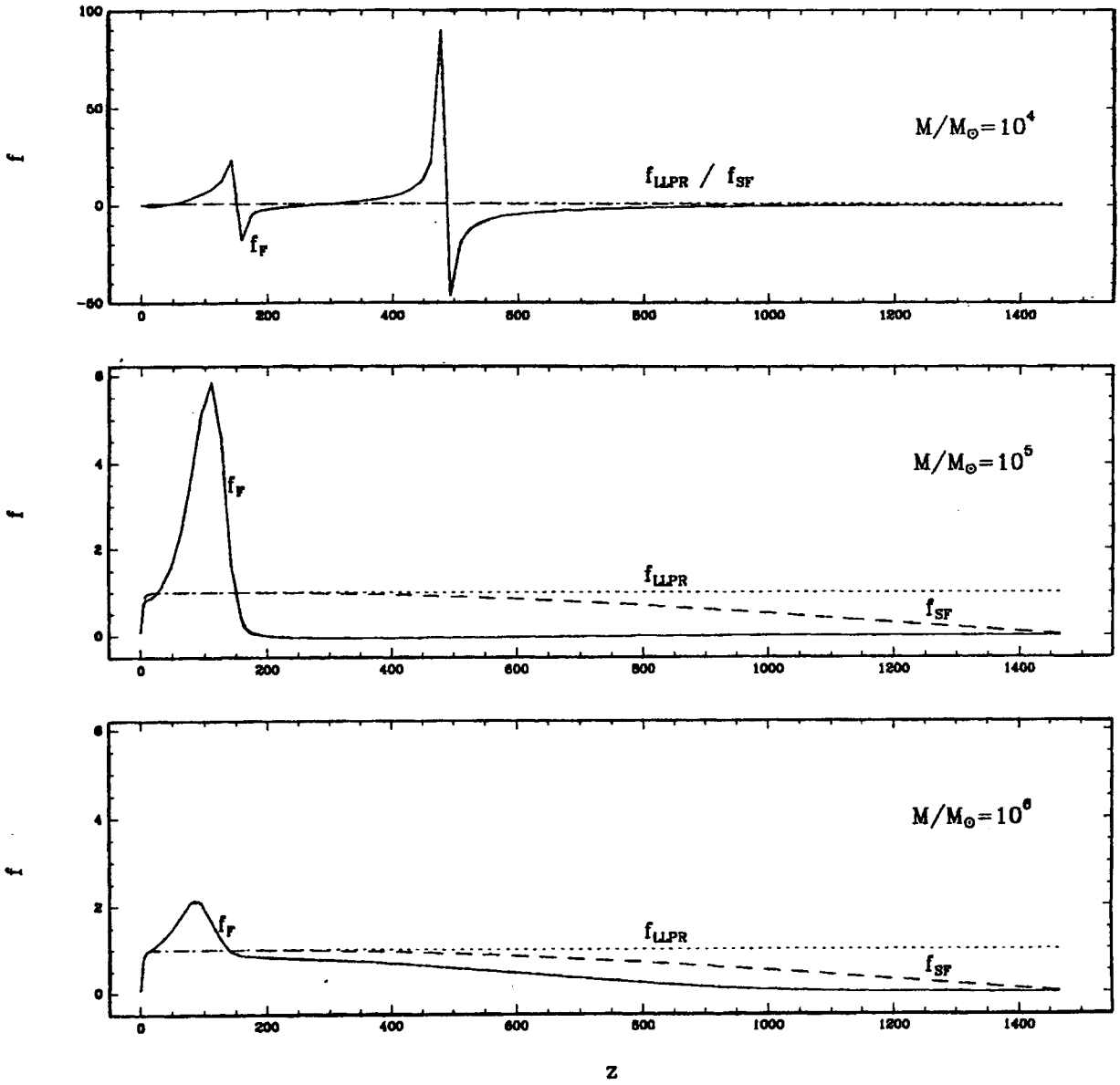

Figure 5. Same as Fig. 1 but for model E, where $\Omega_0=0.01$, $\lambda=0.99$ and $h_0=1.0$.

maximum, and then asymptotically goes over to f_{SF} for very small z.

The behaviour of f_F at high z is due mainly to the photon drag that strongly damps the perturbations. However, for small z the cooling sources become important, helping the growth of density perturbations. For $z \lesssim 300$ the cooling mechanisms reach their maximum efficiency by the formation of hydrogen molecules. These cooling mechanisms prevent the internal pressure to delay the collapse, making the perturbation grow quickly.

For the models with $\Omega_0 = 0.1$ (models B and C), the cosmological constant has little effect on f, but with $\Omega_0 = 0.01$ (models D and E) f is very sensitive to the presence of the cosmological constant.

The influence of the physical mechanisms on the growth of the perturbations is enhanced by the presence of the cosmological constant. Let us compare models C and E (Figs 3 and 5, respectively) that have non-zero λ, but small Ω, with model A (Fig. 1) with $\lambda = 0$ but with the largest density parameter. For cases C and E, f_F reaches a larger maximum than in the case of model A. This can be explained remembering that a non-zero λ increases the age of the Universe and therefore increases the influence of the physical mechanisms. Particularly at late times (small z), having more time with a non-zero λ, there is a greater production of hydrogen molecules, which increases the cooling of the cloud, favouring the growth of the perturbation.

In the case of $M = 10^4\ M_\odot$ for models D and E, the mass of the cloud is smaller than the Jeans mass at the recombination era, meaning that the perturbation evolves as an oscillation. This reflects on the behaviour of f_F ($= d \ln \delta / d \ln a$), which shows peaks arising from the changes in $d\delta/da$.

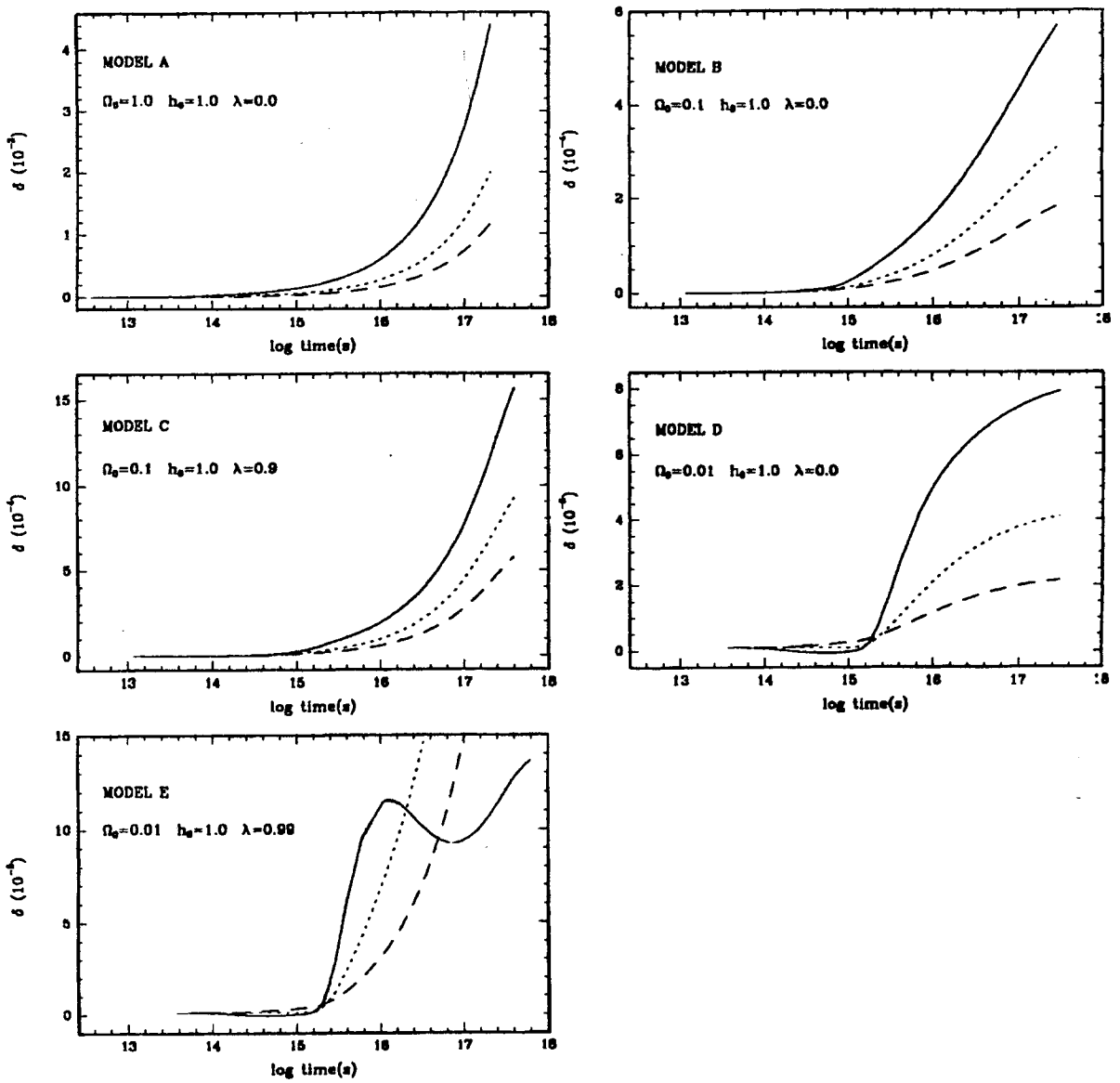

Figure 6. The evolution of δ as a function of the time for Models A, B, C, D and E, with $M = 10^4\ M_\odot$ (solid curve), $M = 10^5\ M_\odot$ (dotted curve), and $M = 10^6\ M_\odot$ (dashed curve).

The evolution of δ as a function of the time, t, can be seen in Fig. 6. This figures shows the temporal evolution for the five models: solid curve, $M=10^4\,M_\odot$; dotted curve, $M=10^5\,M_\odot$; and dashed curve $M=10^6\,M_\odot$. These graphs show that the presence of a cosmological constant is important in the evolution of the clouds, mainly in the models of a Universe with little matter (models D and E).

6 CONCLUSIONS

We studied the effect of physical mechanisms and a cosmological constant on the evolution of primordial clouds, using as an example an initial perturbation $\delta_i=10^{-6}$ for cloud masses 10^4, 10^5 and $10^6\,M_\odot$. Our results compared with the interesting result found by LLPR are summarized as follows.

(1) The physical mechanisms have a great influence on the evolution of the density perturbations, in particular for $z>10$.

(2) For models with $\Omega_0=0.1$, the influence of λ is small, but for the models with minimal matter, $\Omega_0=0.01$, the evolution of the perturbation is very sensitive to the presence of λ.

(3) For small z, λ is important with or without physical mechanisms.

(4) For $\Omega_0=1.0$ and $\lambda=0$, for $\Omega_0=0.1$ and $\lambda=0$ and for $\Omega_0=0.1$ and $\lambda=0.9$, whereas the maximum value of $f_{\rm LLPR}(\max)\simeq 1$, we have for: (1) $M=10^4\,M_\odot$, $f_{\rm F}(\max)\simeq 2$; (2) $M=10^5\,M_\odot$, $f_{\rm F}(\max)\simeq 1.7$; and (3) $M=10^6\,M_\odot$, $f_{\rm F}(\max)\simeq 1.2$.

(5) For $\Omega_0=0.01$ and $\lambda=0$, whereas $f_{\rm LLPR}(\max)\sim 1$, we have for $M=10^5\,M_\odot$, $f_{\rm F}(\max)\sim 3.1$. Similarly, for $\Omega_0=0.01$ and $\lambda=0.99$, we have for $M=10^5\,M_\odot$, $f_{\rm F}(\max)\sim 5.5$.

In general we find that $f_{\rm LLPR}$ is bigger than $f_{\rm SF}$ and $f_{\rm F}$ immediately after the recombination era ($300<z<1400$) since LLPR assumed only the growing mode which has a finite velocity of growth at the recombination era. Initially, $f_{\rm SF}>f_{\rm F}$, since photon drag in $f_{\rm F}$ prevents the growth of $f_{\rm F}$. However, for late z ($z\lesssim 300$) $f_{\rm F}$ becomes bigger than both $f_{\rm LLPR}$ and $f_{\rm SF}$ because the cooling processes in $f_{\rm F}$ helps the growth of the perturbation. $f_{\rm F}$ reaches larger values for non-zero λ, since non-zero λ increases the time in which the cooling mechanisms can act (in particular hydrogen molecules), which helps the growth of the perturbation.

Finally, we note that in the above calculations we used a very small initial perturbation $\delta_i=10^{-6}$. Using an initial perturbation $\delta_i>10^{-6}$ amplifies the effects noted in this paper. The effects of $\delta_i>10^{-6}$ will be presented in a future publication.

ACKNOWLEDGMENTS

The authors thank the Brazilian agencies CNPq (RO, JCNA) and CAPES/PICD (NP) for support. The authors would also like to thank the referee, P. B. Lilje, for helpful comments.

REFERENCES

Barrow J.D., Saich P., 1993, MNRAS, 262, 717
Carlberg R. G., 1981, MNRAS, 197, 1021
Carroll S. M., Press W. H., Turner E. L., 1992, ARA&A, 30, 499
Davis M., Tonry J., Huchra J., Latham D. W., 1980, ApJ, 238, L113
de Araujo J. C. N., 1990, PhD thesis, IAG-Univ. São Paulo
de Araujo J. C. N., Opher R., 1988, MNRAS, 231, 923
de Araujo J. C. N., Opher R., 1989, MNRAS, 239, 371
de Araujo J. C. N., Opher R., 1990, ApJ, 350, 502
de Araujo J. C. N., Opher R., 1994, ApJ, 437, 556
Heath D., 1977, MNRAS, 179, 351
Lahav O., Lilje P. B., Primack J. R., Rees M. J., 1991, MNRAS, 251, 128 (LLPR)
Lepp S., Shull J. M., 1983, ApJ, 279, 578
Lightman A. P., Schechter P. L., 1990, ApJS, 74, 831
Martel H., 1991, ApJ, 366, 353
Peebles P. J. E., 1968, ApJ, 153, 1
Peebles P. J. E., 1980, The Large-Scale Structure of the Universe. Princeton University Press, Princeton NJ
Peebles P. J. E., 1984, ApJ, 284, 439
Press W.H., Teukolsky S. A., Vetterling W. T., Flannery B. P., 1992, Numerical Recipes. Cambridge University Press, Cambridge
Weinberg S., 1972, Gravitation and Cosmology. John Wiley & Sons, New York